



Saral GDR Quality Assessment Report

Cycle 127

04-02-2019 / 11-03-2019

Prepared by :	G.Jettou , CLS F. Piras , CLS	
Accepted by :	DT/AQM , CLS	
Approved by :	F. Bignalet-Cazalet , CNES	



1. Introduction

1.1. Document overview

The purpose of this document is to report the major features that characterize the quality of Saral/AltiKa's data. It is released on a cyclic basis following data dissemination.

The objectives of this document are:

- To provide a quality assessment of Saral/AltiKa GDRs (over ocean).
- To provide users with necessary information for data processing.
- To report any changes likely to impact data quality at any level, from instrument status to software configuration.
- To show the main results for the current cycle.

1.2. Software version

This cycle has been produced with the following Processing Software references :

L1 library=V4.7, L2 library=V5.5p2, Processing Pilot=V5-2p2

The results presented in this report have been performed over GDR products in version T (using patch2).

Several flags or algorithms are not yet tuned and have to be used with caution. A detailed description of the products can be found in the Saral/AltiKa user handbook ([2]). The details of patch2 are listed in [section Content of Patch2](#).

- Note that two inclination maneuvers took place during cycle 6, which brought Saral/AltiKa to the Envisat repeat ground track (inclination around 81.50°).
- Note that since cycle 25, POE-E orbit standard has been applied.
- The Mean Sea Surface used to compute Sea Level Anomaly is :
 - MEAN_SEA_SURFACE.MODEL.CNESCLS11 for cycle 1 to 33,
 - MEAN_SEA_SURFACE.MODEL.CNESCLS15 from cycle 34 onwards.
- Note that the repetitive ground track phase ends on cycle 35, the drifting phase starts cycle 100.
- Note that Jason-2's data distribution stopped at cycle 506, hence the comparisons to Jason-2 will be suspended until further notice.

1.3. Information about tracking mode

Saral/AltiKa is able to track the signal with several onboard tracker algorithms: Median, EDP (Earliest Detectable Part) and Diode/DEM. Median mode is similar to the one used by Envisat and for most cycles of Jason-2. EDP tracker should improve the tracker behavior above continental ice surfaces and hydrological zones. The analysis conducted during the commissioning phase concluded that the median mode is better in average. Finally, Diode/DEM mode is a technique using information coming from Diode and a digital elevation model available onboard. It was already tested on Jason-2. For more information about the various onboard tracker algorithms see [5].

The information about the acquisition / tracking mode used is available in the GDR products (fields `alt_state_flag_acq_mode_40hz` and `alt_state_flag_tracking_mode_40hz`).

During this cycle, Saral/AltiKa used the following acquisition/tracking modes:

- Passes 1 to 1002 : DIODE acquisition / median tracking

Saral GDR Quality Assessment Report **Cycle 127** 04-02-2019 / 11-03-2019
SALP-RP-P2-EA-22250-CLS127

1.4. Cycle quality and performances

During this cycle mispointing has reached levels that has not been observed since the pre-SHM period (September 2014). These levels of mispointing are due to attitude deviation, and explains the higher percentage of missing measurements (see section 2.1). Data quality is severely impacted by these events, a large number of measurements are rejected through the validation process due to mispointing (see section 2.2).

Users are advised to use data with `off_nadir_angle < 0.09deg`

Cycle 127	
Expected number of measurements over ocean	1956522
Percentage of missing measurements	5.66 %
Number of available measurements	1845824
Percentage of rejected measurements	50.95 %
Rejected due to ice	16.65 %
Rejected with threshold verification	40.97 %
Crossover standard deviation	6.72 cm.
Crossover standard deviation on geographical selection ¹	5.29 cm
Sea Level Anomaly standard deviation	10.05 cm
Sea Level Anomaly standard deviation on geographical selection ¹	9.10 cm

Table 1: Summary of cycle 127 performances.

- The standard deviation of Sea Level Anomalies (SLA) relative to the mean sea surface is 10.05 cm. When using geographical selection¹ it lowers down to 9.10 cm .
- Analysis of crossovers and sea surface variability indicate that system performances are close to the usual values obtained with Jason-2/Jason-3's data.
For this cycle, the crossover standard deviation is 6.72 cm. When using geographical selection¹ it lowers down to 5.29 cm .
Performances related to crossover differences are detailed in the dedicated [section Crossover statistics](#).
- Detailed CALVAL results are presented in [section 3](#).

During this cycle HD mode was activated during 1s on the:

- 12/02/2019 at 22:16:47
- 13/02/2019 at 10:40:08
- 28/02/2019 at 22:17:26
- 01/03/2019 at 10:40:46.

¹ Selection to remove shallow waters (1000 m), areas of high ocean variability and high latitudes (> |50|°)

2. Data coverage and edited measurements

This section shows the main results that illustrate the quality of SARAL/Altika's GDR products during this cycle. The following verifications are systematically run on a cyclic basis, which eventually gives access to long term monitoring of missing and edited measurements.

2.1. Missing measurements

Cycle 127 has 44 missing passes and some passes have a large number of missing measurements due to attitude deviation.

Pass number	1	2	3	4	5	6-23	24
% of missing measurements	12,13 %	71,18 %	19,75 %	89,15 %	28,08 %	100 %	31,44 %
Pass number	34	35	36-46	66	67	68	69
% of missing measurements	22,49 %	45,19 %	100 %	14,47 %	20,94 %	58,57 %	98,80 %
Pass number	70	71	94	95	111	113	114
% of missing measurements	100 %	58,73 %	12,93 %	10,94 %	10,00 %	17,92 %	48,26 %
Pass number	115	116	117	152	239	240-248	259
% of missing measurements	31,48 %	38,19 %	47,38 %	10,37 %	19,74 %	100 %	12,76 %
Pass number	260	261	262	263	264	265	266-270
% of missing measurements	12,48 %	24,53 %	31,53 %	44,10 %	53,80 %	68,00 %	100 %
Pass number	271	296	382	407	409	410	451
% of missing measurements	48,55 %	13,13 %	14,14 %	12,92 %	13,58 %	15,09 %	14,56 %
Pass number	453	479					
% of missing measurements	12,45 %	10,13 %					

Table 2: Summary of high rate missing measurements sections.

Missing measurements (relative to a theoretical nominal ground track) are shown figure 1.

The map illustrates missing 1Hz measurements in the GDRs, with respect to a 1Hz sampling of the nominal track of 1002 passes. A part from the missing sections of tracks explained by attitude deviation, usual missing measurements occur over land, essentially over regions with high relief. This is mainly related to altimeter tracking performances over sloping terrain.

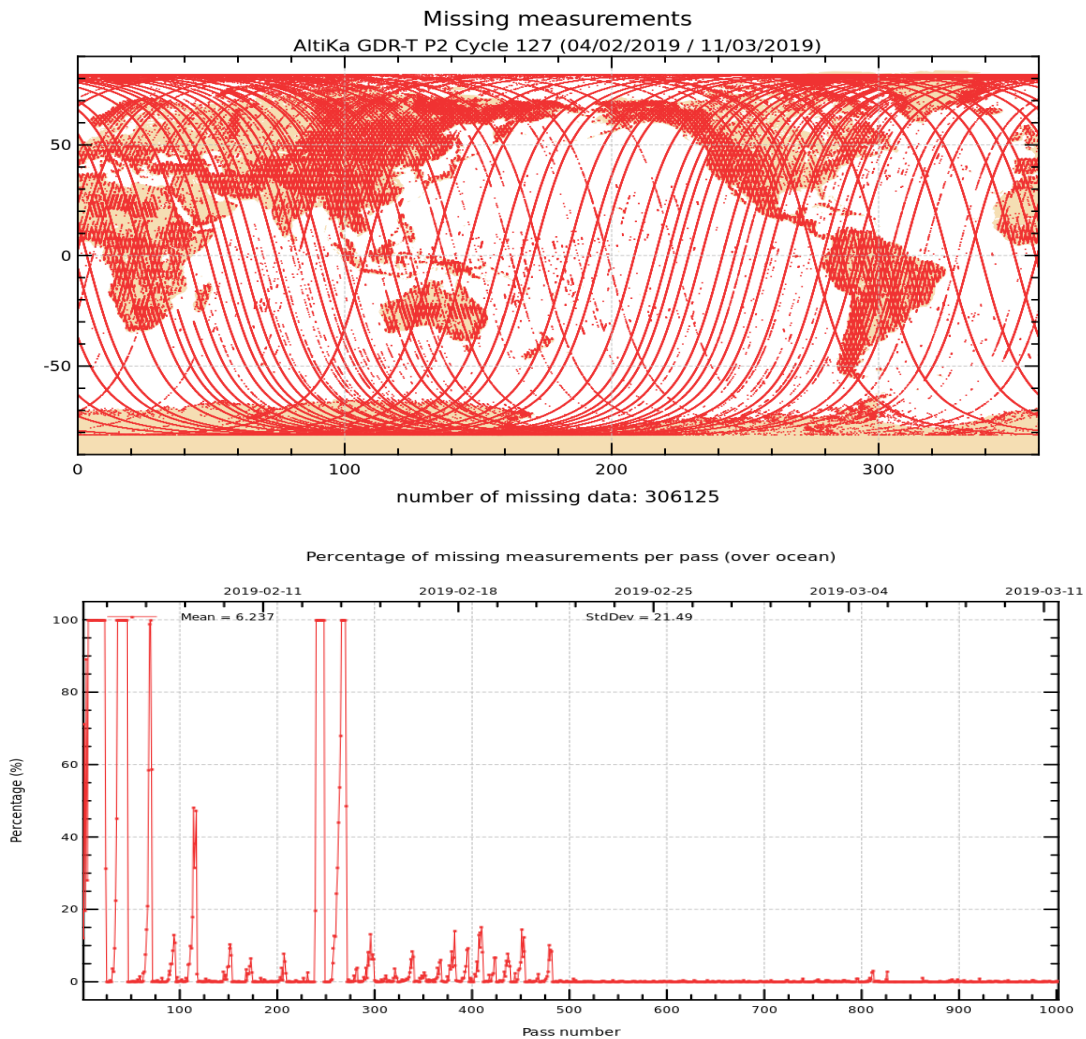


Figure 1: Map of missing measurements for cycle 127 on top. Monitoring of percentage of missing ocean measurements per pass on bottom.

2.2. Edited measurements

Editing criteria are defined for the GDR product in Saral/AltiKa Product Handbook [2].

The editing criteria are defined as a minimum and a maximum threshold for various parameter. Measurements are rejected if one parameter does not lie within those thresholds. These thresholds are expected to remain constant throughout the mission, so that monitoring the number of edited measurements allows a survey of data quality.

In the following, only measurements over ocean are surveyed. It is done by keeping all the data which `surface_type` is equal to 0 (+ the Caspian Sea).

One should bear in mind that this selection has no impact on the global performance (land + ocean) since the most significant results are derived from analyses in open ocean areas.

The number and percentage of removed points are given for each criterion on the following table. Note that these statistics are obtained using measurements already edited by ice flag, that has already removed 16.65 % of ocean points.

Parameters	Min thresh- old	Max threshold	Unit	Nb removed	% re- moved	% mean
Sea surface height	-130	100	m	93228	6.11	0.47
Sea level anomaly	-2	2	m	430264	28.22	0.80
Nb measurements of range	20	DV		139036	9.12	1.11
Std. deviation of range	0	0.2	m	485445	31.84	1.48
Square off nadir angle	-0.2	0.0625	deg ²	606821	39.80	0.31
Dry tropospheric correction	-2.5	-1.9	m	0	0.00	0.00
Combined atmospheric correction	-2	2	m	0	0.00	0.00
MWR wet tropospheric correction	-0.5	0	m	103394	6.78	0.06
Significant wave height	0	11	m	434397	28.49	0.38
Sea State Bias	-0.5	0.0025	m	50118	3.29	0.29
Backscatter coefficient	3	30	dB	266198	17.46	0.34
Nb measurements of sigma0	20	DV		134056	8.79	1.04
Std. deviation of sigma0	0	1	dB	65492	4.30	0.93
Ocean tide	-5	5	m	2467	0.16	0.18
Equilibrium tide	-0.5	0.5	m	2421	0.16	0.17
Earth tide	-1	1	m	0	0.00	0.00
Pole tide	-0.15	0.15	m	0	0.00	0.00
Altimeter wind speed	0	30	m/s	50115	3.29	0.29
Global statistics of edited measurements by thresholds	–	–	–	624763	40.97	2.53

Table 3: Table of parameters used for editing. ' % mean ' is the mean percentage of removed points computed over the 8 first cycles (are highlighted the % of rejected measurements that are more than twice as high a usual).

The measurements rejected during the editing process are shown in figure 2. A part from usual ice-covered and disturbed sea state areas, unexpected high editing rates are observed due to mispointing events (see figure 3).

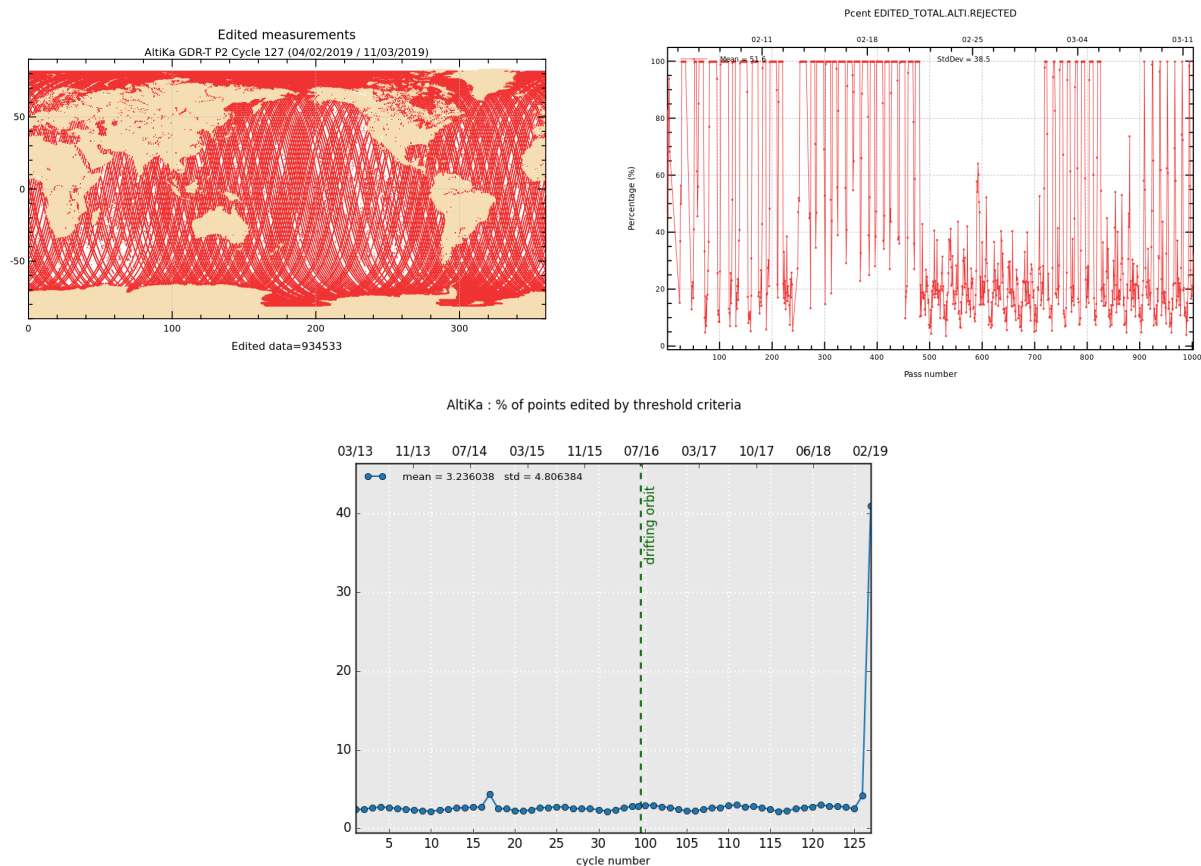


Figure 2: Rejected measurements on thresholds criteria : Cycle 127, map and monitoring of % of rejected measurements per track (top), whole time serie / % of rejected measurements per cycle (bottom).

During this cycle mispointing is quite larger than usual as shown in figure 3). It explains the higher percentage of rejected measurements (up to 100%) (see figure 2). This attitude deviation also explains the higher percentage of missing measurements detailed earlier.

Users are advised to use data with $\text{off_nadir_angle} < 0.09\text{deg}^2$

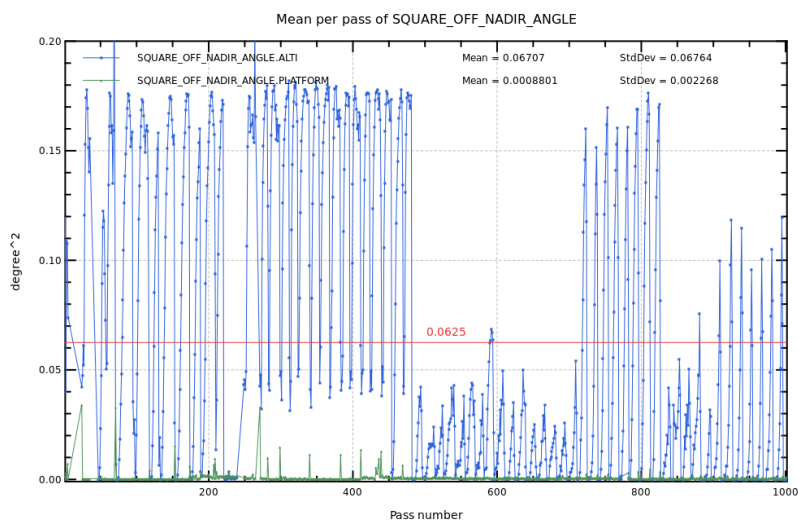


Figure 3: *Mispointing cycle 127.*

3. Instrumental and geophysical parameter analysis

The monitoring of instrumental and geophysical parameters is crucial to detect potential drifts or jumps in long-term time series. The verification of these parameters is very carefully followed up and comparison are often made with Jason-2/Jason-3.

In the following section, only valid data are assessed (validation process detailed in the previous section 2.2).

3.1. AltiKa altimeter and sensor

3.1.1. Sensor status

A detailed assessment of the mission's sensor (AltiKa) is made in a separate bulletin, which is available on request ([7]).

3.1.2. AltiKa altimeter status

This section gives a status of the main instrumental-related variations for the mission's Ka-band altimeter (AltiKa). Two calibration modes are used to monitor the altimeter internal drifts and compute the altimeter parameters. They are programmed about three times per day, over land (desert areas).

The CAL1 mode measures the Point Target Response (PTR) of the altimeter. Among the parameters extracted from the PTR :

- the internal path delay
- the total power of the PTR

The CAL2 mode measures the low pass filter of the altimeter. The evolution of internal path delay and total power of the PTR are plotted to monitor the aging of the altimeter.

Note that in the Saral/AltiKa products, the range is corrected with the internal path delay and the backscatter coefficient takes into account the total power of the measured PTR.

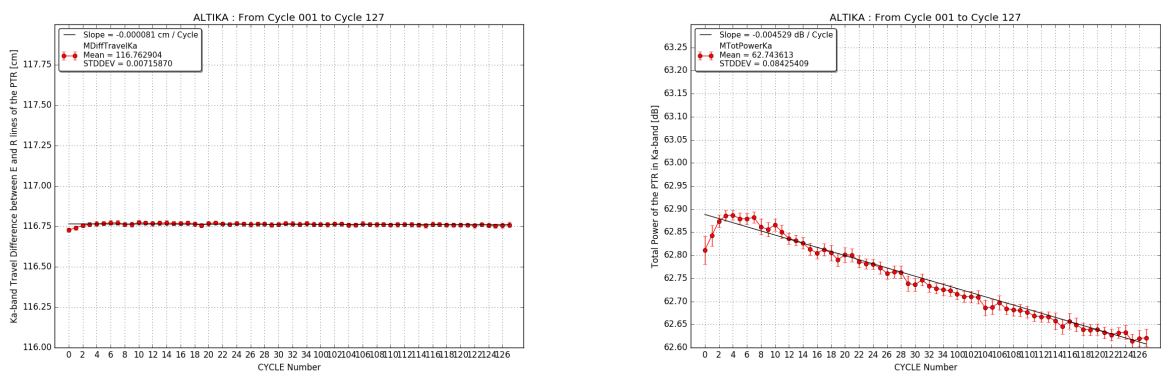


Figure 4: Internal path delay (left) and total power of the PTR (right) for Ka-band.

3.2. Significant wave height

Figure 5 shows wave heights derived from altimeter measurements. SWH data are averaged over a $2^\circ \times 2^\circ$ grid and smoothed afterwards. As shown in the map, wave height can reach several meters.

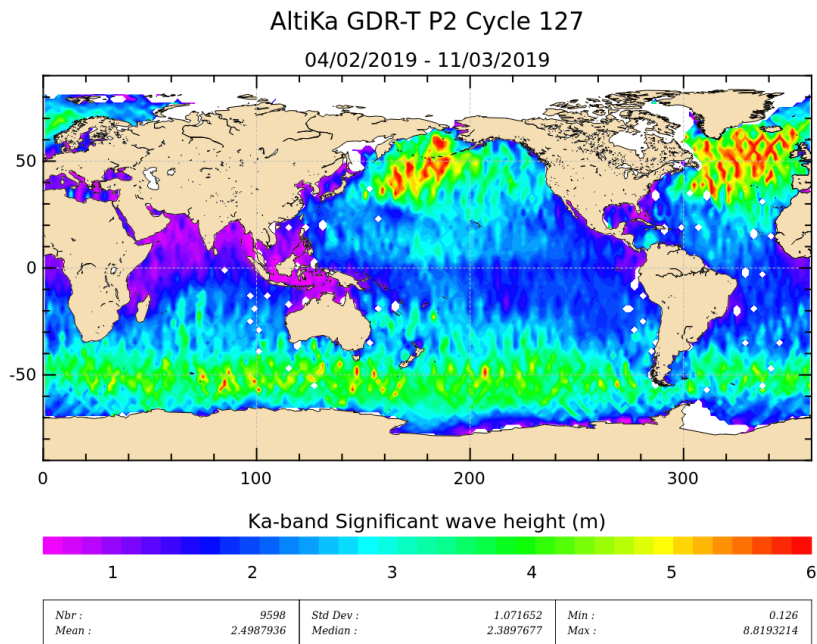


Figure 5: Significant wave height for cycle 127.

The daily average of Ku-band SWH for Jason-2, Jason-3 and Ka-band SWH for Saral/AltiKa is plotted on figure 6.

They show similar features. Note that when computing latitude weighted statistics (not shown here), SARAL/AltiKa significant wave height is generally slightly higher than Jasons' SWH.

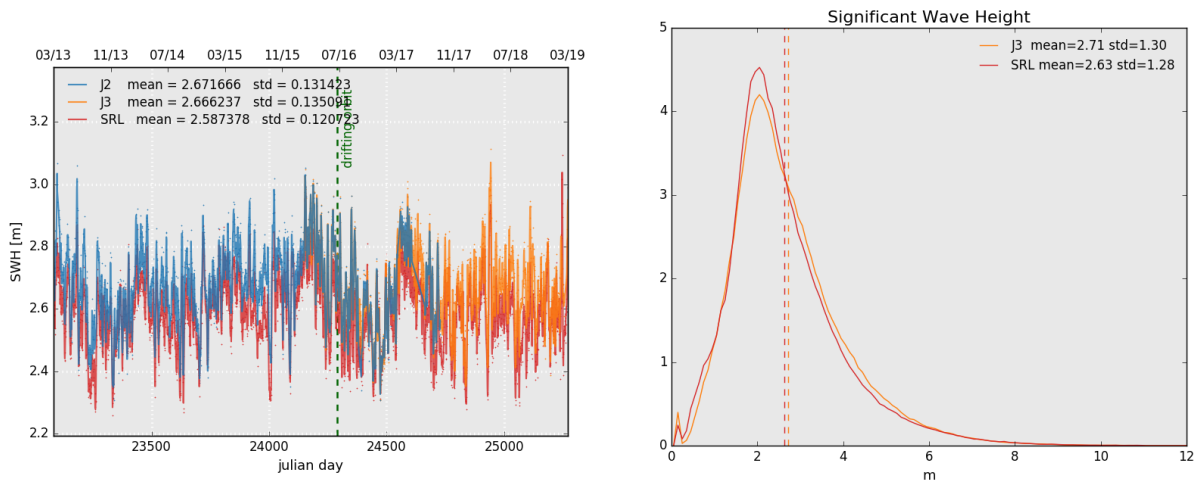


Figure 6: Daily monitoring of significant wave height for AltiKa (Ka-band) Jason-2 and Jason-3 (Ku-band) on the left and histogram for cycle 127 on the right (limited to 66° latitude).

3.3. Backscattering coefficient

The daily average of the backscattering coefficient for Saral/AltiKa (Ka-band), Jason-2 and Jason-3 (Ku-band) is plotted as a function of time on figure 7. Note that due to the different frequencies, Saral/AltiKa backscattering coefficient is not simply shifted by a bias, but their histograms have also different forms. Note that the atmospheric attenuation is available in the Saral/AltiKa products and the backscattering coefficient takes it into account (as it is similarly done for Jason-2 / Jason-3).

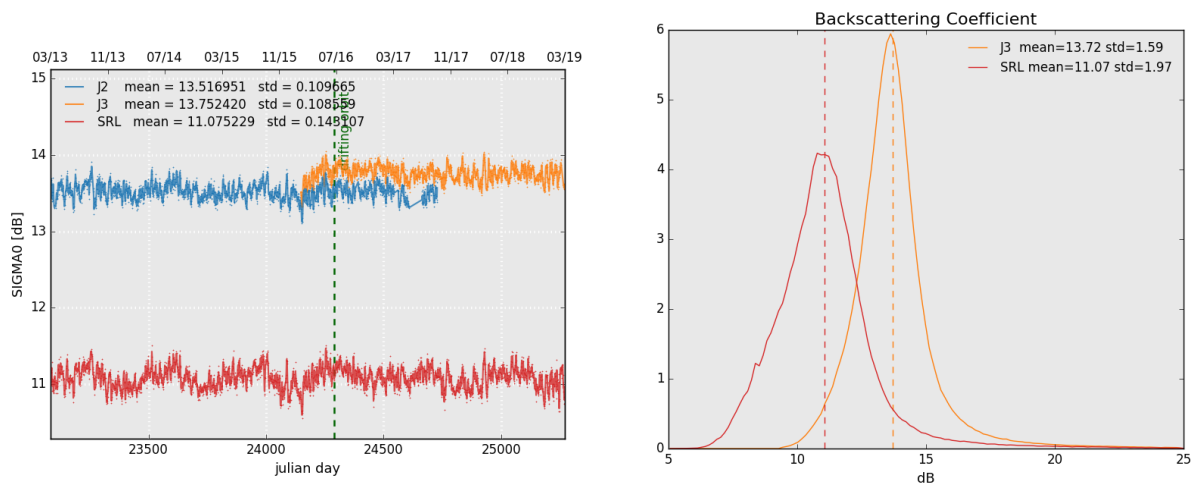


Figure 7: Daily monitoring of backscattering coefficient for Saral/AltiKa, Jason-2 and Jason-3 on the left and histogram for cycle 127 on the right (limited to 66° latitude).

3.4. Ionosphere correction

As Saral/AltiKa has a mono-frequency altimeter in Ka-band, it is not possible to compute a bifrequency ionosphere correction derived from altimeter data. Nevertheless considering only the frequency, the ionosphere correction in Ka-band should approximately be 7 times lower than the one in Ku-band. The daily average of dual-frequency ionosphere correction for Jason-2/3 and GIM ionosphere correction for Saral/AltiKa is plotted on figure 8.

Note that a scale-factor of $(Freq_{Ku}/Freq_{Ka})^2$ was applied to Jason missions values in this figure, in order

to facilitate comparisons between the missions (even though local times and altitude of Jason-2/3 and AltiKa data are not the same).

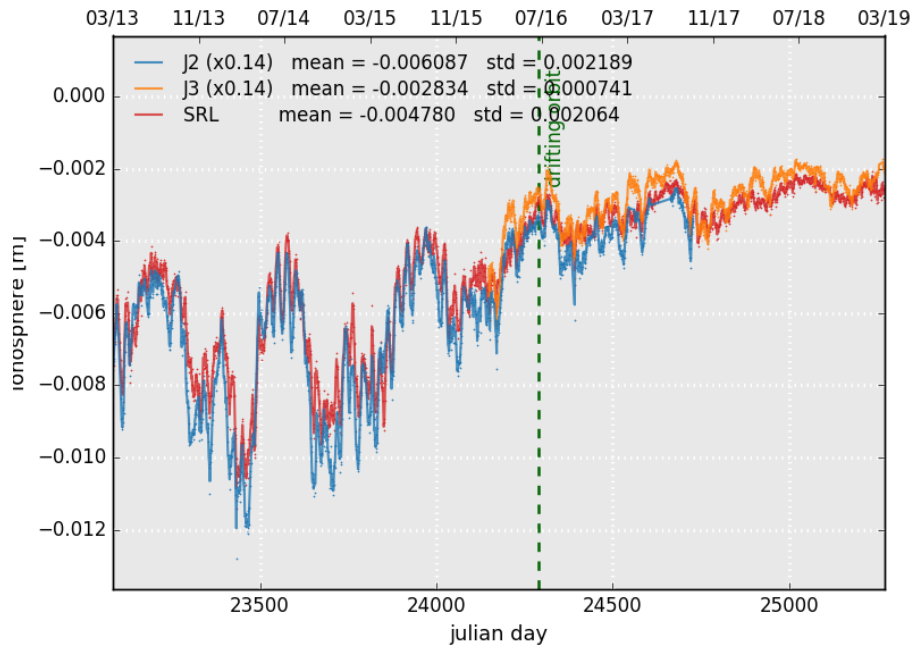


Figure 8: Daily monitoring of dual-frequency ionosphere correction for Jason-2 Jason-3 and GIM ionosphere correction for Saral/AltiKa.

3.5. Altimeter wind speed

Figure 9 shows wind speed estimations derived from altimeter measurements. Data from the current cycle are averaged over a $2^\circ \times 2^\circ$ grid and smoothed afterwards. Altimeter wind speed for AltiKa GDR-T Patch2 version is estimated with the algorithm of Lillibridge et al. [6], which is based on Abdalla wind speed algorithm [3].

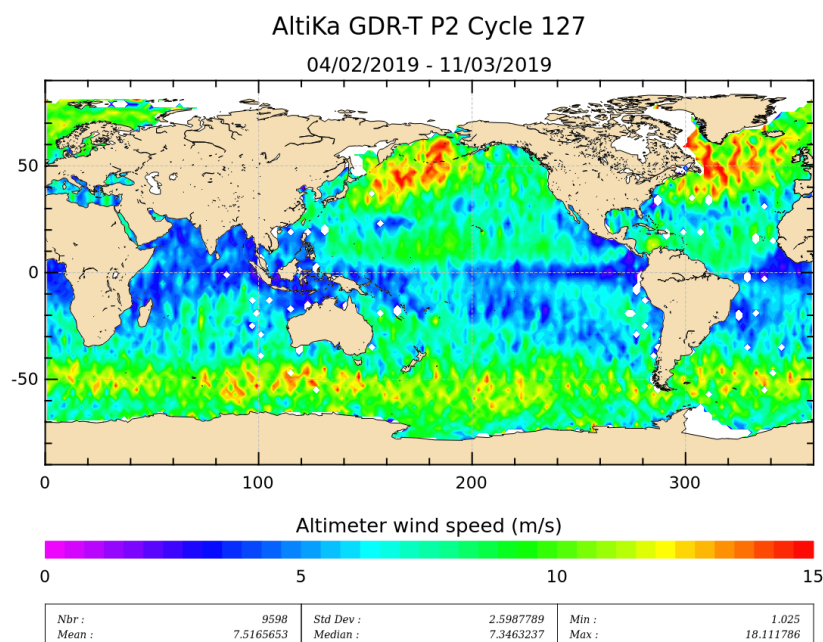


Figure 9: Altimeter wind speed for cycle 127.

The daily average of altimeter wind speed of Saral/AltiKa, Jason-2 and Jason-3 is plotted on the left side of figure 10. The histogram is shown on the right side. AltiKa's wind speed histogram starts around 1 m/s (as other altimeter's wind speeds based on Abdalla's algorithm). A kind of bi-modal behavior can be observed (see also [9]), otherwise Jasons' AltiKa's altimeter wind speed are similar.

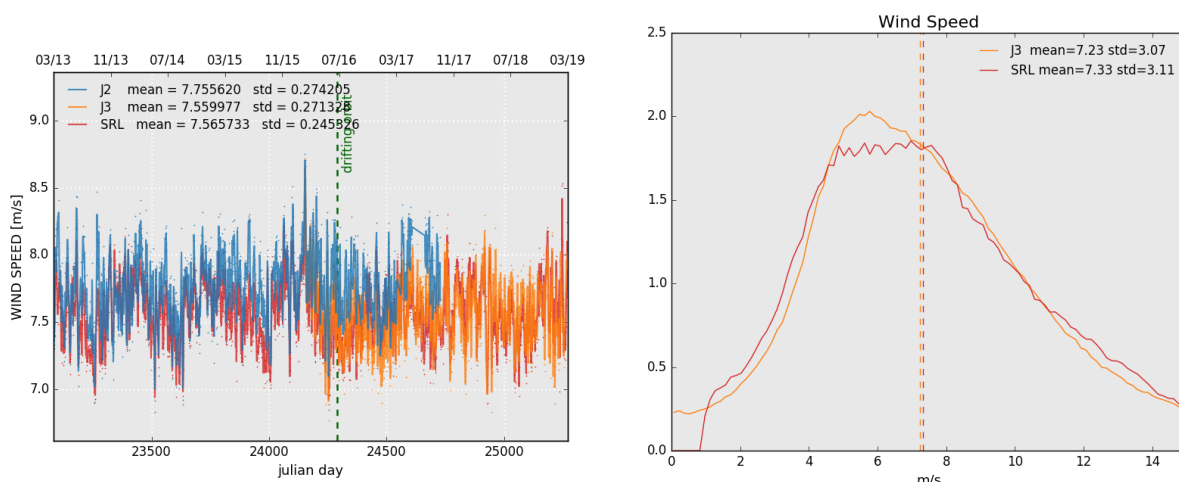


Figure 10: Daily monitoring of altimeter wind speed for Saral/AltiKa, Jason-2 and Jason-3 on the left and histogram for cycle 127 on the right (limited to 66° latitude).

3.6. Radiometer parameters

Figure 11 shows the mean value of wet troposphere correction difference (radiometer - ECMWF) for the current cycle.

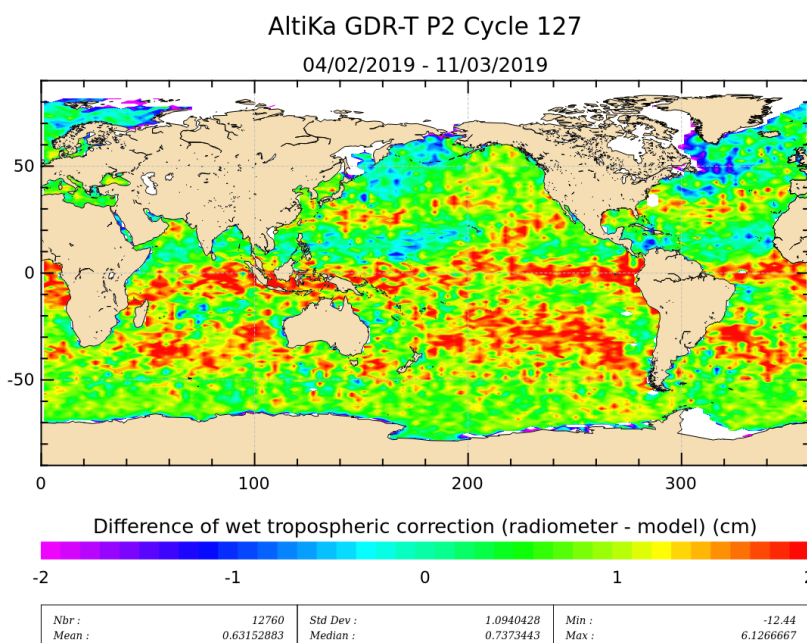


Figure 11: Mean of wet troposphere correction difference (Radiometer-ECMWF model) for cycle 127.

For the current version of GDRs, linear relations have been computed between the measured brightness temperatures and the simulated ones. These linear relations are applied on the 23.8 GHz and 37 GHz channels. Furthermore a bias is applied on the backscattering coefficient while computing radiometer wet troposphere correction.

The radiometer wet troposphere correction is globally quite consistent with the model, but the standard deviation of the difference are quite different between Saral/AltiKa and Jason missions, which is expected

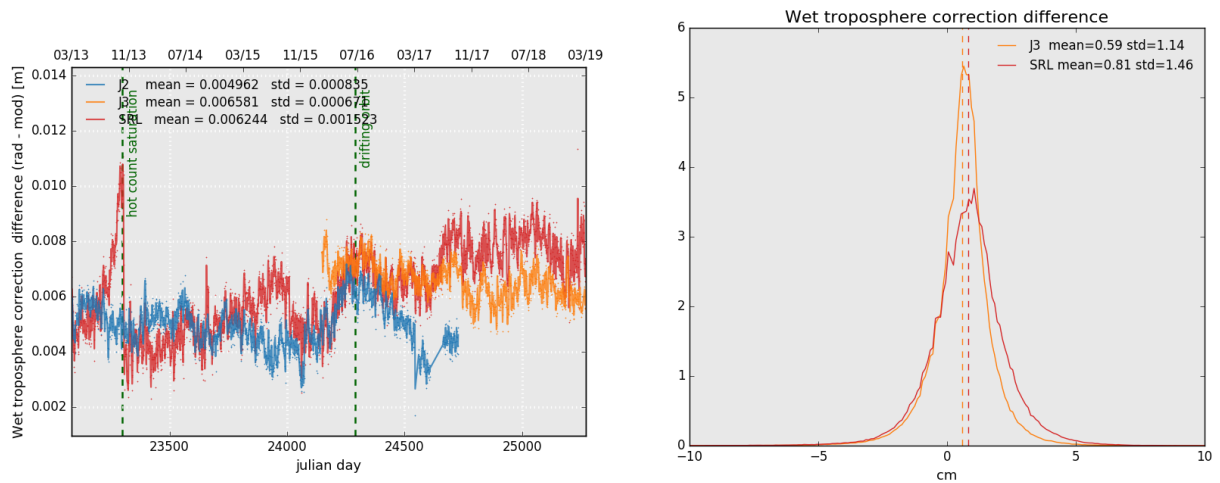


Figure 12: Daily monitoring of wet troposphere differences (Radiometer-ECMWF model) for Saral/AltiKa Jason-2 and Jason-3 (left) and histogram on the right (limited to 66° latitude) for cycle 127 .

since Saral/AltiKa has a Ka band dual-frequency radiometer whereas Jasons have a three-frequency Ku band radiometer.

Note that the standard deviation of the wet troposphere difference is reduced in Patch2 compared to Patch1. Further work is ongoing to improve the retrieval algorithms of the radiometer wet troposphere correction .

Note that in summer/fall 2013 (till 2013-10-22), a saturation of the hot calibration counts occurred, which had an impact on the 37 GHz brightness temperature (and the parameters based on it, see left of figure 12). This was not an instrumental problem, but rather an issue related to onboard parameterization.

3.7. Mispointing

Figure 13 shows the mean value of the mispointing angle for valid measurements (values $< 0.0625deg^2$).

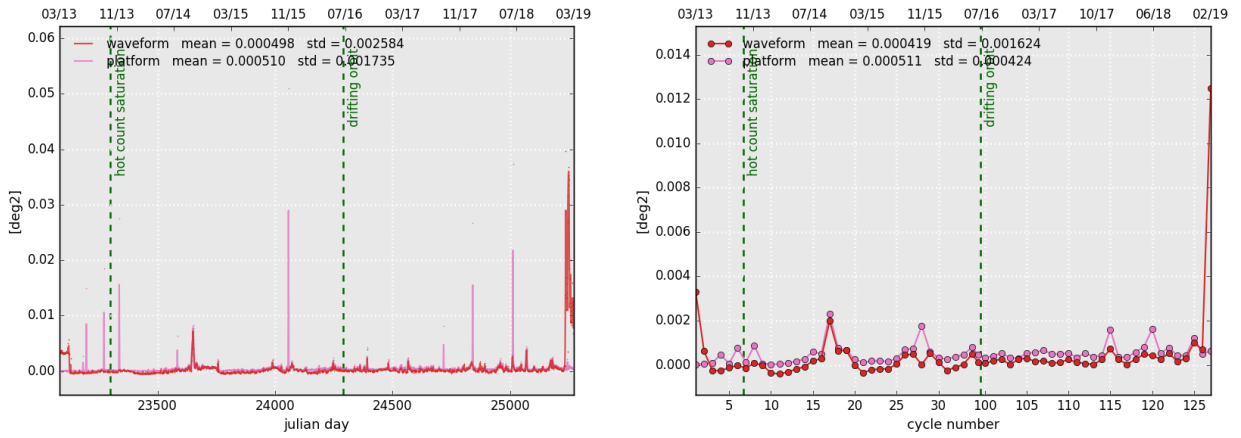


Figure 13: Daily (left) and cyclic (right) monitoring of SARAL/AltiKa's mispointing angle: comparison between the one derived from waveform retracking and the one measured by platform startrackers.

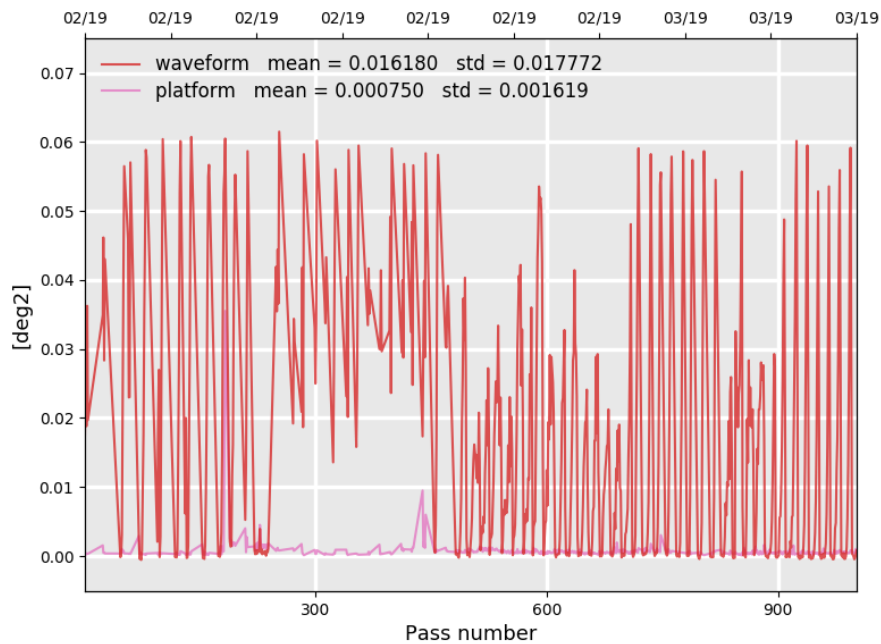


Figure 14: Monitoring per pass for cycle 127 of SARAL/AltiKa's mispointing angle: comparison between the one derived from waveform retracking and the one measured by platform startrackers.

Mispointing angle measured by platform startrackers does not show the mispointing event on cycle 127 because it is due to a startracker issue.

4. Crossover Analysis

4.1. Overview

SSH crossover differences are computed as a difference of SSH values at the crossing point between an ascending and a descending track. Crossover differences are systematically analyzed to estimate the quality of the products and the mission's performances. SSH crossover differences are computed with a valid dataset on a cyclic basis. The tracks time lag cannot exceed 10 days, in order to limit the effects of ocean variability which can be a source of error in the estimation. The mean of SSH crossover differences should be close to zero and standard deviation should ideally be small.

Nevertheless SLA varies also within 10 days, especially in high variability areas. Models of several geophysical corrections are less precise in high latitude due to lower data availability thanks to seasonal ice coverage. Therefore an additional geographical selection - removing shallow waters, areas of high ocean variability and high latitudes ($> |50|^\circ$) - is applied for cyclic monitoring.

In the following section, only valid data are assessed (validation process detailed in the section 2.2).

4.2. Maps of SSH crossover differences

The map of the mean differences at crossovers (averaged over a $4^\circ \times 4^\circ$ grid) is plotted for the current cycle figure 15.

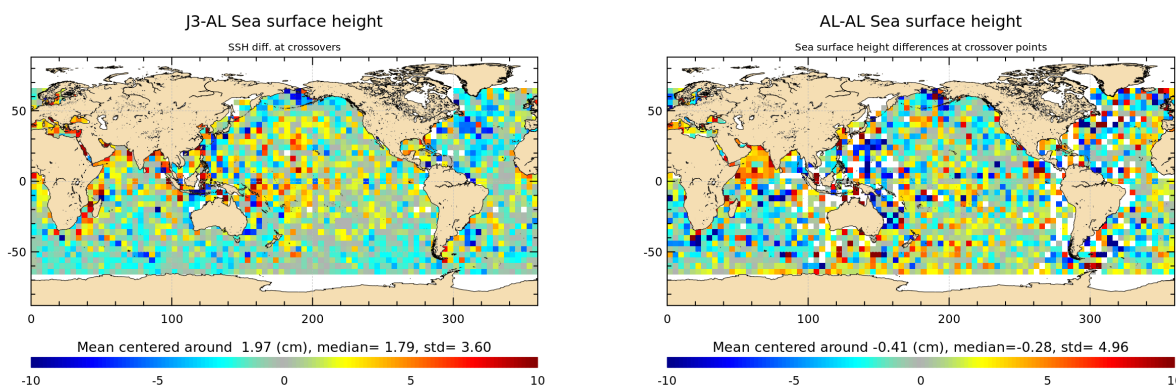


Figure 15: Mean of multi-mission SSH and mono-mission SSH differences at crossovers for cycle 127.

When applying additional geographical selection, removing shallow waters, areas of high ocean variability and high latitudes ($> |50|^\circ$), the mono-mission box-averaged crossovers's standard deviation is of 4.04 cm.

4.3. Cycle by cycle monitoring

The mean and standard deviation of SSH differences at crossovers are plotted for Saral/AltiKa, Jason-2 and Jason-3 as a function of time on top of figure 16. The statistics are computed after data editing and using the geographical selection criteria mentioned earlier, that is to say $|\text{latitude}| < |50|^\circ$, bathymetry < -1000 m, ocean variability (computed over several years) < 0.2 m.

Note that statistics are computed for each cycle based on Saral/AltiKa's cycle numbering. Data number may therefore vary between the missions (due to a different number of missing/edited measurements). The plot at the bottom of figure 16 is computed using the same selection as above, combined to a latitude weighting of the crossovers' SSH differences before estimating the standard deviation. Using this method leads to a

small increase of the standard deviation of SSH differences at crossovers.

This is done in order to reduce the weight of crossover points in high latitudes since there are much more crossover points in high and very high latitudes than in mean and low latitudes, especially for Jasons. This method is based on the crossovers theoretical density described in the SARAL/AltiKa yearly report 2014 [1].

Saral/AltiKa and Jason-2/Jason-3 show similar performances. Using the radiometer wet troposphere correction improves the coherence between ascending and descending tracks (standard deviation of SSH differences at crossovers points is reduced) for Saral/AltiKa and both Jason-2 and Jason-3. Without latitude weighting Saral/AltiKa has slightly better performances than Jason's, with latitude weighting (in order to reduce the weight of the numerous crossover points in high latitudes) their performances are equivalent.

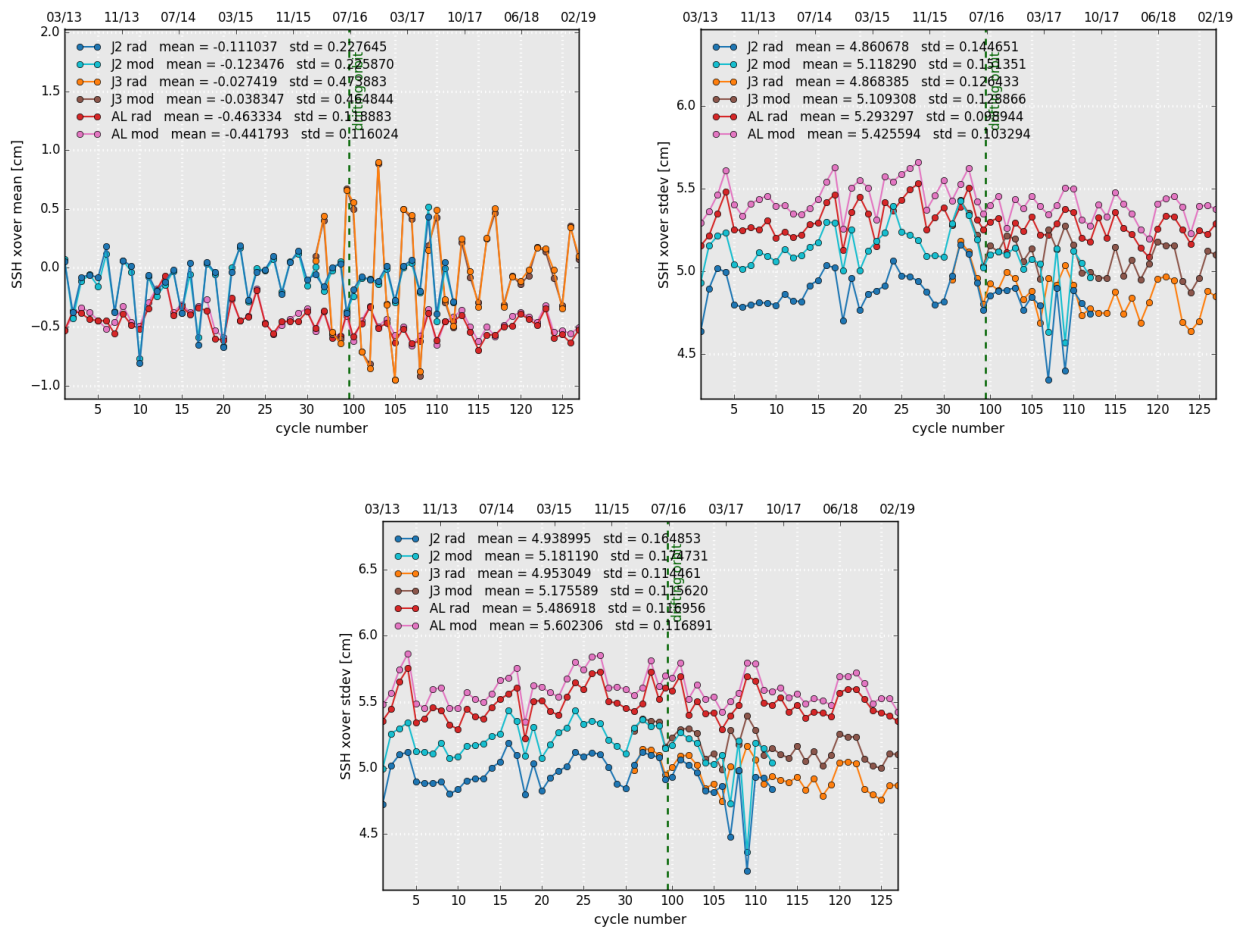


Figure 16: *Cyclic monitoring of mean (left) and standard deviation of SSH differences at crossovers using only the geographical selection criteria (right) and both geographical selection and latitude weighting (bottom).*

Figure 17 shows the mean and the standard deviation of Jason-2 / AltiKa and Jason-3 / AltiKa 10-days SSH crossovers using radiometer wet troposphere correction and ECMWF wet troposphere correction model. The bias between Jason-2 and AltiKa is around 4.6 cm and 1.7 cm between Jason-3 and Saral/AltiKa when using wet troposphere correction model. Using radiometer wet troposphere correction reduces the standard deviation at multi-mission crossover points (right of figure 17).

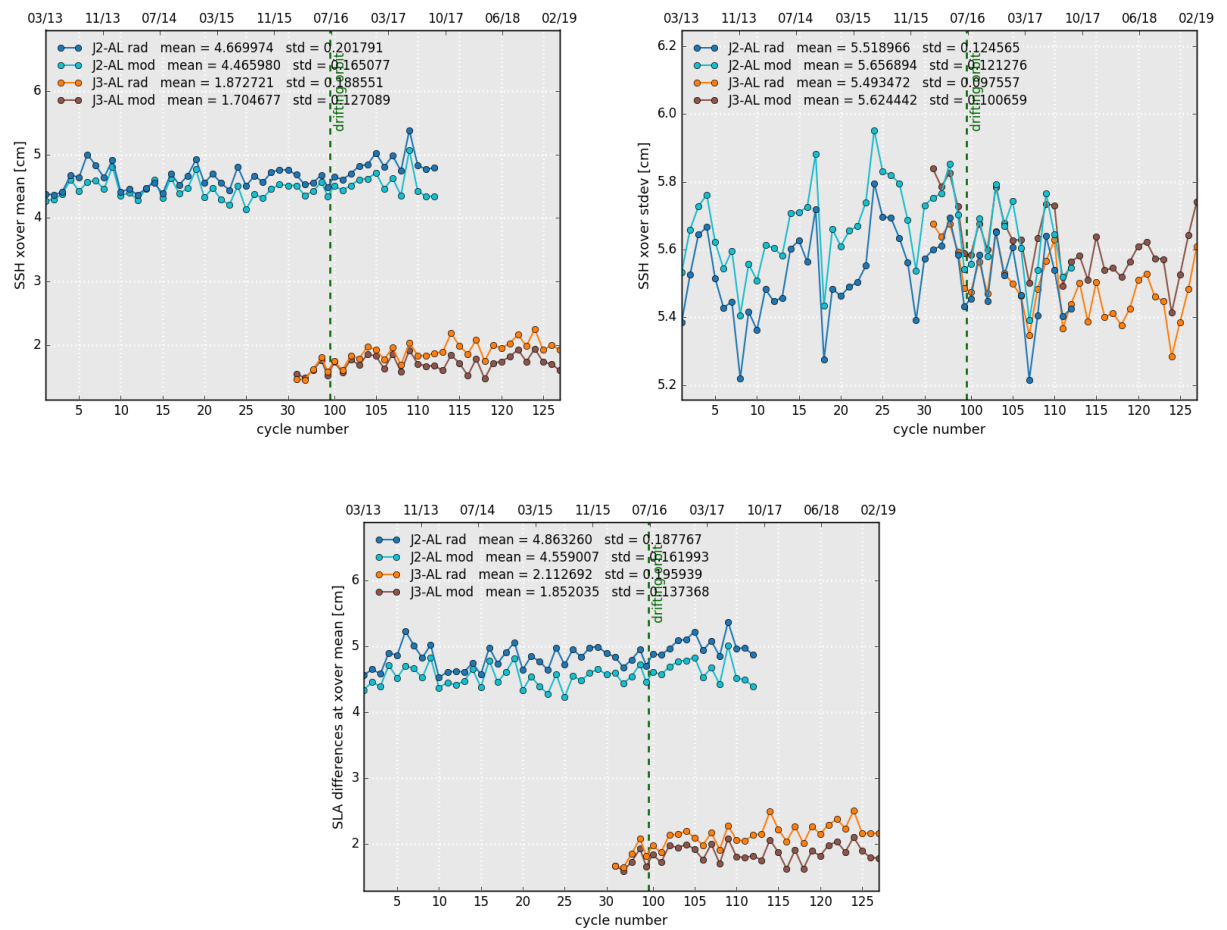


Figure 17: Cyclic monitoring of mean (left) and standard deviation (right) of Jason-2 / ALtiKa & Jason-3 / ALtiKa SSH differences at crossovers using geographical selections. Box-averaged SLA differences at crossovers (bottom).

4.4. Comparison of pseudo time tag bias

The pseudo time tag bias is found by computing at SSH crossovers a linear regression between the SSH and the satellite radial speed (\dot{H}), also referred to as orbital altitude rate :

$$SSH = \alpha \dot{H}$$

This method allows us to estimate the time tag bias but it absorbs also other errors correlated with \dot{H} as for instance orbit errors. That is why it is called "pseudo" time tag bias.

The Jason satellites had a pseudo datation bias close to -0.28 milliseconds with an approximately 60-days signal. The origin of this pseudo time tag bias of the Jason satellites was found by CNES in 2010 [4]. It has a mean of about -0.25 milliseconds and is dependent on the altitude of the satellite. For Jason-2 GDR-D data, the datation was directly modified in order to correct it properly, whereas for Jason-1 GDR-C product it is taken into account thanks to a correction (pseudo_datation_bias_corr_ku). Therefore the average of the pseudo datation bias is now close to zero for the Jason satellites, nevertheless the periodic signal remains and is not yet explained.

Figure 18 shows the monitoring of the pseudo datation bias for Saral/AltiKa (35 days), Jason-2 (10 days) and Jason-3 (10 days) on a cyclic basis. Saral/AltiKa shows a small negative pseudo time-tag bias.

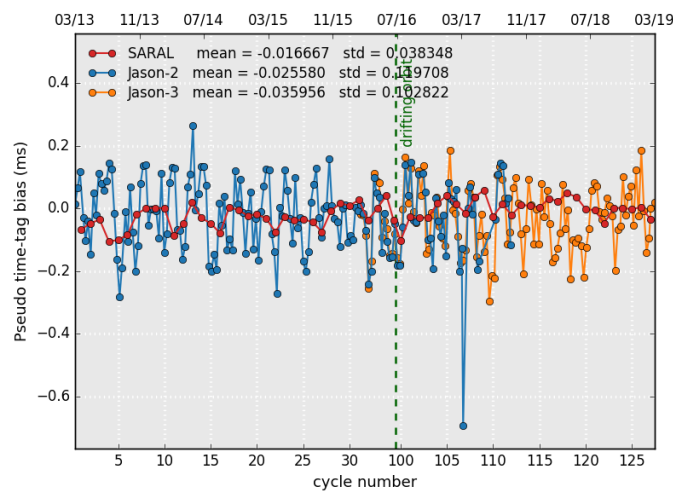


Figure 18: Cyclic monitoring of pseudo time tag bias for Saral/AltiKa.

5. Along track analysis

In the following section, only valid data are assessed (validation process detailed in the section 2.2).

5.1. Sea Level Anomaly

5.1.1. Temporal analysis

The monitoring of mean SLA for Saral/AltiKa Jason-2 and Jason-3 is presented on figure 19 left. The mean bias between Saral/AltiKa and Jason-2 is around 4.9 cm whereas it is around 2.9 cm between Saral/AltiKa and Jason-3 (when using model wet troposphere correction). Note that the mean sea surface standard has evolved to an improved version on cycle 34, resulting in a visible 2.5 cm drop in the mean SLA.

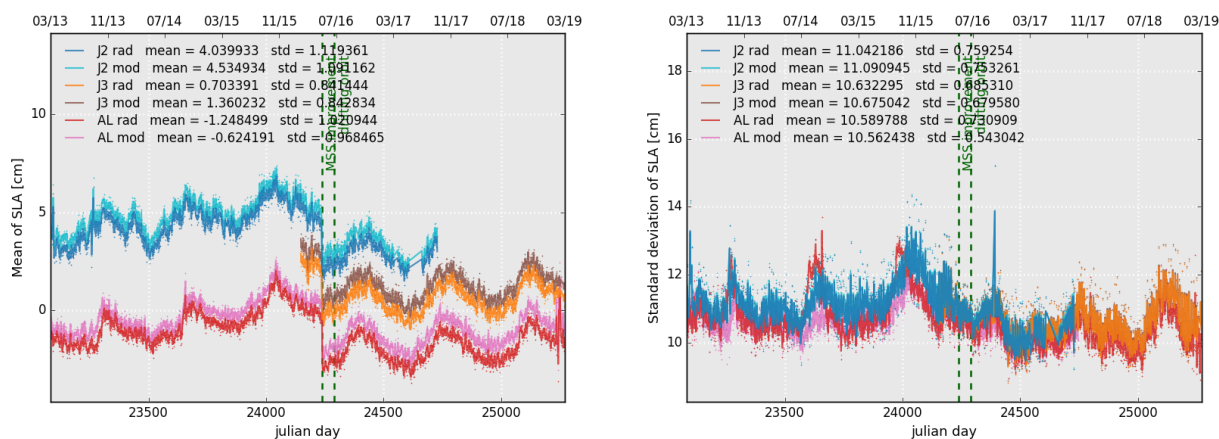


Figure 19: Daily monitoring of the mean (right) and standard deviation (left) of SLA for Saral/AltiKa, Jason-2 and Jason-3.

5.1.2. Maps

Figure 20 shows the map of Saral/AltiKa's SLA.

Figure 21 permits to point out areas where the SLA is higher than 30 cm (after editing and centering the data). A part from isolated points, high SLA are as expected located in high ocean variability areas.

As Saral/AltiKa and Jasons are not on the same ground track SLA measurements are first averaged over the same grid to compute SLA differences between the missions.

This difference is quite noisy for one cycle (see left of figure 22), since sea state varies a lot especially in regions of high ocean variability. Right side of these figures shows therefore an average over several cycles, the maps are less noisy indeed, and high variability regions as Gulf Stream and Antarctic circumpolar current are still visible.

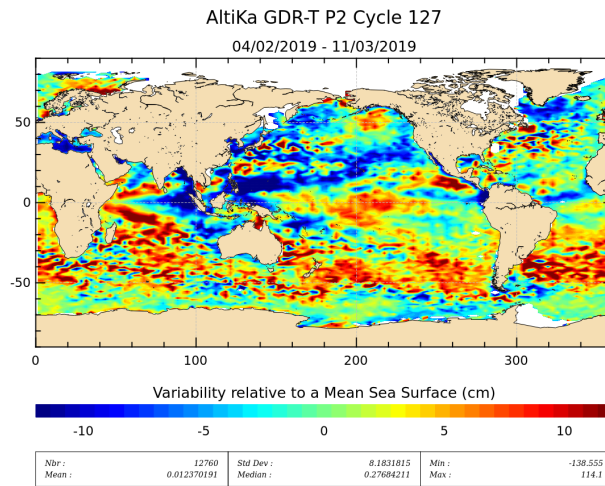


Figure 20: *Sea level anomaly relative to MSS for cycle 127.*

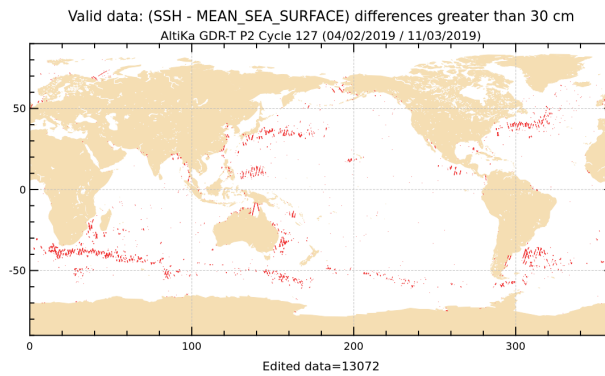


Figure 21: *SLA higher than 30 cm for cycle 127.*

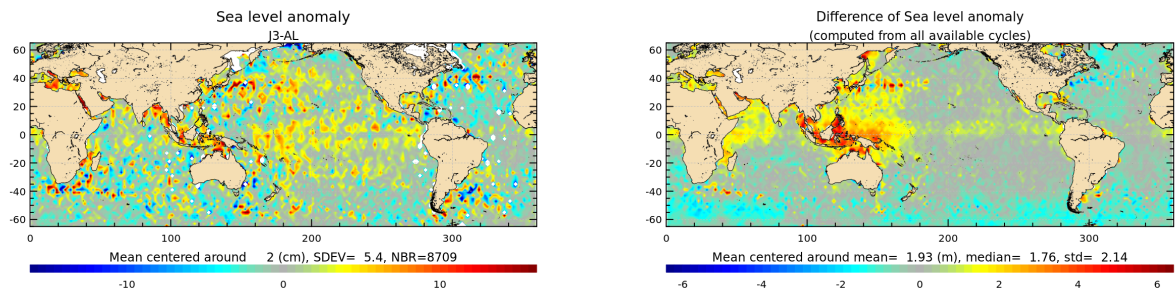


Figure 22: *Jason-3 – Saral/AltiKa SLA differences for cycle 127 (left) and averaged over the whole Saral/AltiKa period (right).*

6. Content of Patch1

Hereafter the content of Patch1 is recalled. IGDR data were produced with this patch from cycle 4 pass 395 onwards till cycle 10 pass 565.

Altimeter calibration file : The altimeter calibration stability has been analyzed. Based on the actual data, we have implemented an averaging of the calibrations over a 7 days window for the low pass filter (identical to Jason-2) and 3 days for the internal path delay and total power (not used on Jason-2). This will slightly reduce the daily noise observed in the altimeter calibration data.

Altimeter characterization file : We have updated the altimeter characterization file using the flight calibration of the gain values (4 calibrations performed). The impact is very small (of the order of 0.01 dB).

Retracking look-up tables : We have updated the ocean retracking look-up tables using the flight calibration data (PTR). The impact is very small on the range and sigma0 values but of the order of 15 cms on SWH for low sea states.

MQE : We have analyzed the altimeter flight data and based on the observed MQE values over ocean a threshold of $2.3E-3$ (Jason-2 value is $8E-3$) is used for the 1Hz data computation.

Neural network : A first linear relation has been computed between the measured BT and the simulated one. This linear relation is applied on the 23.8 GHz only – the same analysis will be conducted on the 37 GHz and sigma0. This generates a bias on the radiometer wet tropospheric correction which is now much more consistent with the model one.

Atmospheric attenuation : The value outputted by the neural algorithm is now recorded in the level2 products (it was set to 0 at the beginning of the mission). Rad_water_vapor and rad_liquid_water: The values have been corrected to comply with the actual unit in the level2 products (kg/m^2). But the rad_liquid_water remains not reliable as an anomaly has been noticed in the neural network.

SSHA : The radiometer wet tropospheric correction is now used to compute this value (the model value was used at the beginning of the mission).

Controls parameters : The threshold values have been updated with the flight data. This is a first tuning – additional work is necessary.

7. Content of Patch2

Hereafter the content of Patch2 is recalled. All GDR data were produced or reprocessed (cycles 1 to 7) with this patch in order to have a homogeneous dataset, whereas IGDR data were only produced with this patch from cycle 10 pass 566 onwards.

Wind look-up table : The table provided by NOAA is used. This table is only based on the measured σ_0 , taking into account the atmospheric attenuation (σ_0 at the surface). (Reference: Lillibridge et al. [6])

SSB look-up table : The table provided by R. Scharroo is used (same method as in [8]). We use only the significant wave height to compute the SSB.

Radiometer neural algorithm : Taking into account several months of AltiKa measurements, the neural network coefficients have been updated. Note that this modifies the radiometer related parameters (radiometer wet troposphere correction, atmospheric attenuation, radiometer liquid water content and radiometer water vapor content).

Ice-2 retracking algorithm : The algorithm has been updated taking into account the AltiKa Ka band specificities (ice2 algorithm was based on ENVISAT Ku band experience).

FES2012 tide model : This new tide model is included, improving the SSH accuracy in coastal zones. (Reference : www.avisio.altimetry.fr/en/data/products/auxiliary-products/global-tidefes2description-fes2012.html).

Matching pursuit algorithm : The algorithm based on J. Tournadre proposal has been tuned to comply to AltiKa Ka band specificities.

MQE parameter scale factor : The scale factor of the MQE has been modified.

Update of the altimeter characterization file : The altimeter characterization file has been modified in order to account for 63 values of altimeter gain control loop (AGC). This has impacts over sea ice and land hydrology, in some cases the AGC was set to default value in current P1 products.

Doris on ground processing (Triode) : The Doris navigator ground processing has been upgraded to reduce the periodic signal observed on the altitude differences with MOE/POE.

Equilibrium long-period ocean tide height : The equilibrium long-period ocean tide height (`ocean_tide_equil`) is now at default values over land, but also lakes and inland seas (such as Caspian Sea). Furthermore some ocean data close to land are also at default value. As the geocentric ocean tide height (`ocean_tide_sol1`) includes `ocean_tide_equil`, `ocean_tide_sol1` is also at default value in the same places as `ocean_tide_equil`.

Non-equilibrium long-period ocean tide height : The non-equilibrium long-period ocean tide height (`ocean_tide_non_equil`) of Patch2 is different from the one in Patch1, as it is now computed with FES2012 algorithm, instead of previously FES2004 algorithm.

8. References

References

- [1] Prandi, P., V. Pignot and S. Philipps, 2015, Saral/ AltiKa validation and cross calibration activities (Annual report 2014), SALP-RP-MA-EA-22418-CLS
- [2] SARAL/AltiKa Products handbook, December 2013 *SALP-MU-M-OP-15984-CN* edition 2.4. Available at: http://www.aviso.altimetry.fr/fileadmin/documents/data/tools/SARAL_Altika_products_handbook.pdf
- [3] Abdalla, S., 2007. Ku-band radar altimeter surface wind speed algorithm. *Proc. of the 2007 Envisat Symposium*, Montreux, Switzerland, 23-27, April 2007, Eur. Space Agency Spec. Publ., ESA SP-636.
- [4] Boy, François and Jean-Damien Desjonqueres. 2010. Note technique datation de l'instant de reflexion des échos altimètres pour POSEIDON2 et POSEIDON3 *Reference: TP3-JPOS3-NT-1616-CNES*
- [5] J.-D. Desjonqueres, G. Carayon, N. Steunou, and J. Lambin, 2010. Poseidon 3 Radar Altimeter: New Modes and In-Flight Performances. *Marine Geodesy*, **33(S1)**, 53-79. See: <http://www.tandfonline.com/doi/abs/10.1080/01490419.2010.488970#.UjBdPLzCwUE>
- [6] Lillibridge, J., Scharroo, R., Abdalla, S., and Vandemark, D. (2013) One-and Two-Dimensional Wind Speed Models for Ka-band Altimetry. *Journal of Atmospheric and Oceanic Technology*. doi: <http://dx.doi.org/10.1175/JTECH-D-13-00167.1>
- [7] J. Poisson et al.: AltiKa Instrument Quality Assessment Report Cycle 127. SALP-RP-MA-EA-22233-CLS-127.
- [8] Scharroo, R., and J. L. Lillibridge. Non-parametric sea-state bias models and their relevance to sea level change studies, in *Proceedings of the 2004 Envisat & ERS Symposium*, Eur. Space Agency Spec. Publ., ESA SP-572, edited by H. Lacoste and L. Ouwehand, 2005.
- [9] R. Scharroo, J. Lillibridge, S. Abdalla, and D. Vandemark. Early look at SARAL/AltiKa data. Oral presentation at OSTST 2013, Boulder, USA. Available at http://www.aviso.altimetry.fr/fileadmin/documents/OSTST/2013/oral/Scharroo_Early_look_at_SARAL.pdf